ALGINATE AFFECTING THE CHARACTERISTICS OF POROUS β-TCP/ALGINATE COMPOSITE SCAFFOLDS

F. AFRIANI [a,*], K. DAHLAN[a], S. NIKMATIN[a], O. ZUAS[b]
[a]*Laboratory of Biophysics, Faculty of Mathematics and Natural Sciences, Bogor Institute of Agriculture. Jl. Raya Dramaga, 16680, West Java, Indonesia*
[b]*Research Centre for Chemistry, Indonesian Institute of Science (RCChem-LIPI), Kawasan PUSPIPTEK Serpong, 15314 Tangerang, Banten, Indonesia*

In this study, a β-tricalcium phosphate (β-TCP) has been successfully prepared from eggshell waste. The prepared β-TCP was then used as a precursor for the synthesis of porous β-TCP/alginate composite scaffold using $CaCl_2$ as crosslink agent. The existence of alginate on the β-TCP/alginate composite scaffolds was confirmed by observing their structural and morphological properties using X-ray diffraction (XRD), Fourier transform infrared spectroscopy (FTIR), scanning electron microscopy (SEM), and micro-computed tomography (μ-CT scan). The XRD and FTIR data show that there was no effect of alginate addition on the phase transformation of either β-TCP or alginate structure. On the other hand, SEM and μ-CT scan indicate that the alginate was significantly influence in term of pore size and porosity of the synthesized β-TCP/alginate composite scaffold. The pore size and porosity of the synthesized composite scaffold were found in the ranges of about 224.17 – 322.29 μm and 61.6 – 68.8%, respectively. Based on the findings of this study, it can be concluded that all synthesized β-TCP/alginate composite scaffolds have desirable property where they met the criteria as an ideal pore size for bone regeneration application.

(Received July 9, 2015; Accepted September 11, 2015)

Keywords: Porous scaffold, Eggshell, β-tricalcium phosphate, Alginate, Freeze-drying.

1. Introduction

The use of porous scaffolds (a three-dimensional substrate) in tissue engineering for bone therapy process is a promising alternative in biomedical field [1]. In addition to osteoconductivity property, for bone therapy, a biocompatibility and biodegradability, as well as pore size of a porous scaffold are very important role for the migration process and supply of nutrients during a growing cell process [2]. For scaffold application, preparation of porous scaffold having ideal pore with size ranging between 100-400 μm is intended to meet the requirements for the process of colonization, proliferation, and penetration of cells [3, 4].

In the research area of composite scaffold, β-tricalcium phosphate (β-TCP) is one of the most promising materials for the synthesis of scaffold and it has been studied extensively. The advantage of the β-TCP is not only due to its ability of accelerating the bone treatment process but also can be used as material in the development of polymer composite-based scaffold. In term of its flexibility property, the polymer composite-based scaffold is better than pure brittle ceramic scaffolds [5, 6]. Moreover, another attractive material in the area of synthesis of ceramic/polymer composite scaffold is alginate. Alginate is an anionic polysaccharide which consists of two main monomers i.e., β-D-mannuronic acid and α-L-gluronic acid. The alginate is found in a wide variety of brown seaweed. The alginate is an interesting precursor because the alginate hydrogel is easy to be stabilized by only replacing its Na^{2+} with another cation such Ca^{2+} [8, 9]. Besides, the alginate could induce the formation of a composite scaffold with a desirable pore size which

*Corresponding author: fitriafriani25@yahoo.com

greater than 100 μm [7]. In the biomedical field, the alginate is considered to many application, including wound healing and tissue engineering [10], as well as drug delivery [11]. Especially for bone injuries treatment, the alginate is considered to be more biocompatible, non-toxic, and relatively low cost. Besides, the alginate is potential to be developed because the alginate can be introduced into body with a minimum invasive manner and fill the irregular bone defects, as well as support cells regeneration [9]. However alginate shows poor mechanical properties, therefore, its application by composing with other potential materials is highly required. Some studies dealing with the use of alginate as a composite material for the synthesis of porous composite scaffold have been reported including chitosan/alginate/nano-silica [12], hydroxyapatite/chitosan-alginate [13], and calcium sulfate/alginate [14].

To date, a number of methods for the fabrication synthesis of porous scaffold have been reported, namely, porogen replication method [15, 16], foaming method [17], and freeze-drying method [18]. Among these methods, freeze drying method is preferred for the fabrication of a 3D porous scaffold because of its simplicity. In this freeze drying method, the pores creation of the composite scaffold are firstly induced by the ice crystals formation followed by the ice crystal removal lead to holes creation when the sample is dried under low temperature condition [19].

The purpose of this study was to evaluate the effect of alginate on the porous β-TCP/alginate composite scaffold synthesized using freeze-drying method. In the synthesis process, the β-TCP powder and alginate were used as composite scaffold precursors. The effects of alginate variation at different ratio of β-TCP powder to alginate were evaluated. The β-TCP powder prepared from chicken eggshell was not only chosen because of its high calcium carbonate content (~94%) and its interesting properties as mentioned above, but also its availability as abundant materials in Indonesia (approximately 129,919.9 tonnes in 2014) [20]. The effect of alginate were evaluated by characterizing the synthesized of β-TCP/alginate composite scaffold using X-ray diffraction (XRD) analysis, Fourier transform infrared (FTIR) spectroscopy, scanning electron microscopy (SEM) and micro-computed tomography (μ-CT) scan.

2. Experimental methodology

2.1. Materials

Eggshells were obtained from food restaurant located in Bogor, Indonesia. The following commercially available chemicals were used without further purification, including phosphoric acid (H_3PO_4, 85%, Merck, USA), calcium chloride ($CaCl_2$, >99%, Merck, USA), and alginate (CV. Setia Guna, Indonesia). Double distillate water was used in all experimental runs.

2.2. Procedures

2.2.1. Preparation of CaO

The eggshells were collected and their surfaces were mechanically cleaned. The calcium oxide (CaO) was obtained by calcining the raw cleaned eggshells in oven at 1000^{o}C for 5 h under atmospheric air. The prepared CaO was stored under dry atmosphere condition for further synthesis of β-TCP Powder.

2.2.2. Synthesis of β-TCP powder

The β-TCP powder was synthesized using the following simple procedure. A certain amount of CaO powder was dissolved in double distillate water to make calcium hydroxide ($Ca(OH)_2$) solution. After that, H_3PO_4 was added drop wise onto $Ca(OH)_2$ suspension to form a precipitated $Ca(OH)_2$ suspension. The ratio of calcium (Ca) to phosphate (P) was 1.5. The precipitated suspension was immediately sintered at 1000^{o}C for 7 h to obtain the β-TCP powder. The prepared β-TCP powder was stored under dry atmosphere condition for further use on the synthesis of porous β-TCP/alginate composite scaffold.

2.2.3. Synthesis of porous β-TCP/alginate scaffold

In a typical experiment, a certain amount of the synthesized β-TCP powder was dissolved in double distillate water to form aqueous β-TCP solution. Into aqueous β-TCP solution, alginate

powder was added to form β-TCP-alginate solution mixture. The ratios of β-TCP to alginate were 8:2, 7:3, and 6:4, denoted as TA-82, TA-73, and TA-64, respectively. Moreover, a gelling method was used for cross-linking processes of the TA-82, TA-73, and TA-64. Such cross-linking process lead to gel formation and it was conducted by adding drop by drop a cross-linking solution 0.03M $CaCl_2$ into the TA-82, TA-73, and TA-64 solutions. After that, all the β-TCP/alginate gels obtained were placed in the refrigerator for 12 h. While the final porous β-TCP/alginate scaffolds were obtained by freeze-drying the gels at -40^oC for 19 h.

2.2.4. Scaffold characterizations

For sample characterizations, the XRD data were recorded on a Bruker D8 Advance X-ray at 40 kV and 35 mA with Cu (Kα = 1.5406 Å) as the radiation source. The 2θ was scanned in the range between 20^o – 70^o at a speed of 0.019^o /min. The functional groups in all samples under investigation were recorded on a Shimadzu IR Prestige DSR- 8000 FTIR using potassium bromide (KBr) media in the wavenumber ranging from 400 cm^{-1} to 4000 cm^{-1} at a scanning rate of 4 cm^{-1} /min. The microstructure of the samples was observed using a JEOL JSM-360LA scanning electron microscope (SEM). The porosity of the samples was determined using a SkyScan 1173-micro-computed tomography (μ-CT) scan operated at 45 kV and 80 μA.

3. Results and discussion

3.1. Crystalline property of scaffold

Fig. 1 shows the XRD patterns of the synthesized β-TCP/alginate composite scaffolds. As can been from fig. 1, the XRD of all β-TCP/alginate composite scaffolds have well defined diffraction peaks that are similar to the diffraction peaks of β-TCP database with JCPDS card No. 09-0169. The three highest diffraction peaks at about 27.79^o, 31.02°, and 34.36° are assigned to the peak characteristics of the β-TCP, which are indexed to the 214, 0210, and 220 orientations, respectively. No diffraction peaks arising from any impurity can be detected in the XRD pattern. Nonetheless, small amount of the β-TCP precursors [β-calcium pyrophosphate (β-$Ca_2P_2O_7$) and calcite ($CaCO_3$)] were still observed indicated by their diffraction with low intensity peaks. The presence of these two β-TCP precursors is probably due to their incomplete heating process during calcination and sintering [21].

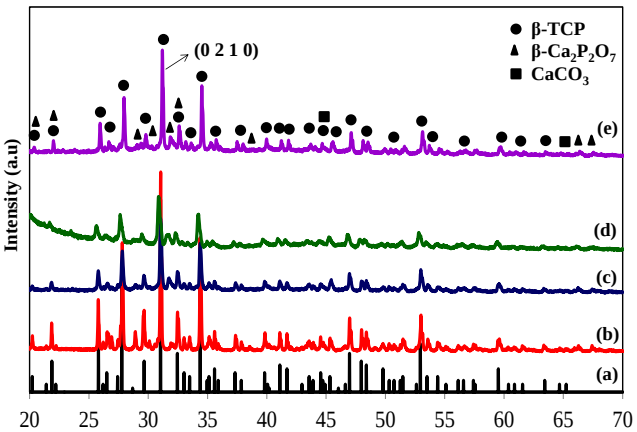

Fig. 1. The XRD pattern of: (a). β-TCP database, (b). β-TCP powder, (c). TA-82, (d). TA-73, and (e) TA-64 composite scaffold. The XRD pattern of both β-TCP powder and β-TCP database with JCPDS Card No. 09-0169 is included for comparison only (For interpretation of the references to colour in this figure, the reader is referred to the web version of the article).

The average crystallite size of the β-TCP powder was calculated from the full-width at half-maximum (FWHM) of (0210) reflection as presented in fig. 1 using Scherrer's formula [22], as shown in Eq. 1.

$$D = {}^{0.9\lambda}/_{\beta\ cos\theta} \quad (1)$$

Where D is the crystallite size (nm), λ is the wavelength of the X-ray diffraction (nm), β is the FWHM (rad), and θ is the angle of diffraction (rad). From the calculation, the average size of crystalline powder of β-TCP was found to be about 75.43 nm. Besides all synthesized β-TCP-based composite scaffolds had good crystal quality indicated by well-defined XRD diffraction peaks. The identified phase of β-TCP phase relative to non β-TCP phase was found to be about 72%. In comparison, there is no different in phase characteristic between β-TCP and β-TCP/alginate can be observed (Fig. 1), indicating that alginate addition had no effect on the new phase formation. In a word, the diffraction peak characteristics of β-TCP were found to be similar to that of β-TCP/alginate composite scaffold. Interestingly, the addition of alginate had significant effect on reduction of the crystallite size of the β-TCP/alginate composite scaffold. The crystallite sizes of the β-TCP/alginate composite scaffold were found to be in the range of 28.10 – 65.9 nm, which is lower than the crystallite size of β-TCP (75.43 nm). Lowering in the crystalline degree of the β-TCP/alginate composite scaffold to values ranging from 58.70 to 66.80% could be the reason for decreasing in their crystallite size in comparison to that of β-TCP powder (72%) [23].

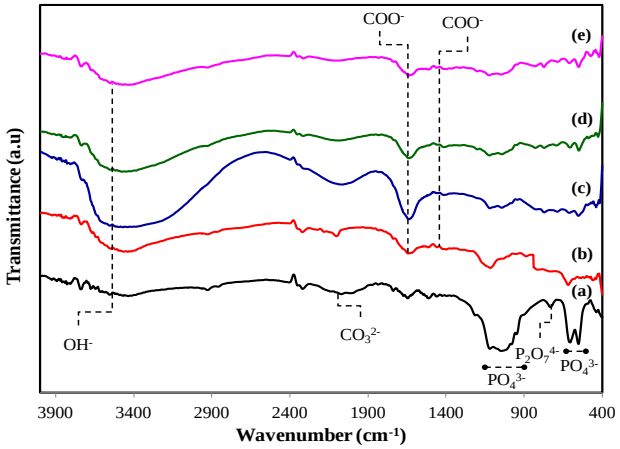

Fig. 2. FTIR spectrum of: a) β-TCP powder, b) alginate, c) TA-82, d) TA-73, and e) TA-64 (For interpretation of the references to colour in this figure, the reader is referred to the web version of the article).

3.2. Infrared spectroscopy

Fig. 2 displays the FTIR spectra of the β-TCP powder, alginate and synthesized β-TCP/alginate composite scaffolds. From the spectra of β-TCP powder (Fig. 2a), it can be observed that the FTIR spectrum shows some absorption bands at about 550 cm^{-1}; 605 cm^{-1}; 945 cm^{-1}; 977 cm^{-1}; 1045 cm^{-1}; and 1118 cm^{-1}. All these bands are typical for functional groups of PO_4^{3-} that are mainly found in β-TCP-based material. In addition, the bands at wave number of 729 cm^{-1} and 2000 cm^{-1} is closely related to the functional group of the $P_2O_7^{4-}$ and CO_3^{2-} originated from calcium pyrosphate and calcite as impurities. Spectrum of alginate (Fig. 2b) is characterized by its vibration asymmetric and symmetric bands of COO^- at wave number of about 1610 cm^{-1} and 1413 cm^{-1} [24, 25]. These entire bands spectrum are in agreement with the FTIR spectrum of β-TCP powders reported in the literature [26]. It is clearly observed that the all synthesized composite scaffolds indicate typical absorption band that show a combination of β-TCP and alginate. Moreover, the spectra of β-TCP/alginate composite scaffolds are shown in fig. 2c-e. It was noticeable that all characteristic bands spectra found in all synthesized composite scaffolds (Fig.

2c-e) are similar to that in both β-TCP (Fig. 2a) and alginate (Fig. 2b). In addition, no other bands of functional group originated from new materials can be found, indicating that the β-TCP/alginate composite scaffolds were formed via physic interaction process. The FTIR data is in agreement with the XRD data, where β-TCP and alginate were present in the form of their composites and no other new phases were formed. This phenomena is in line with previous reported study, where the use of freeze-drying method on the synthesis of composite scaffold would not lead to the formation of new functional group because the freeze drying process does not provide enough energy for phase transformation during the synthesis process [27].

Based on the above discussion, a possible mechanism for the formation of the β-TCP/alginate composite scaffold can be suggested as shown in eq. (2) – (6) and fig. 3. The first step for over all the processes was the preparation of β –TCP (β-$Ca_3P_2O_8$) as illustrated in eq. 2-6. In this typical mechanism, the calcite (CaO) powder as a material precursor was prepared by heating the surface cleaned eggshells (Eq. 2), [28]. After that, the CaO powder was diluted into H_2O to form ($Ca(OH)_2$) suspension (Eq. 3). The ($Ca(OH)_2$) suspension was precipitated using H_3PO_4 solution (Eq. 4) followed by sintering at 1000^{o}C for 7 h to obtain β –TCP powder (Eq. 5 - 6), [29].

$$CaCO_3 \rightarrow CaO + CO_{2\uparrow} \quad (2)$$

$$CaO + H_2O \rightarrow Ca(OH)_2 \quad (3)$$

$$2Ca(OH)_2 + 2H_3PO_4 \rightarrow 2CaHPO_4 + 4H_2O \quad (4)$$

$$2CaHPO_4 + 4H_2O \rightarrow \beta\text{-}Ca_2P_2O_7 + H_2O_{\uparrow} \quad (5)$$

$$\beta\text{-}Ca_2P_2O_7 + CaO \rightarrow \beta\text{-}Ca_3P_2O_8 \quad (6)$$

The second step was the synthesis of the β-TCP/alginate composite scaffold, which is schematically shown in fig. 3. At the initial step, water soluble alginate (Na-alginate) solution was mixed with aqueous β-TCP solution (Fig. 3a). Immediately after the mixing process, under ambient temperature, a reaction was occurred between β-TCP and alginate, where β-TCP/alginate hydro-gel was partially formed (the formation of weak alginate hydro-gel was visually observed after the mixing process) (Fig. 3b). Such partial formation of alginate hydro-gel of (Fig. 3b) was probably initiated by interaction between some divalent calcium ion (Ca^{2+}) on β-TCP and oxygen atom on the acid functional group of alginate [9, 30]. After that, $CaCl_2$ cross-linking agent solution [31] was added into β-TCP-alginate hydro-gel. During this cross-linking process, it was expected that the Ca^{2+} from $CaCl_2$ cross-linked agent replaced all remaining Na^+ on alginate to form strong β-TCP/alginate hydro-gel (Fig. 3c). Finally, the β-TCP/alginate composite scaffold as the final product (Fig. 3d) was obtained by removing water from the β-TCP/alginate cross-linked hydro-gel using freeze drying method at -40^{o}C for 19 h.

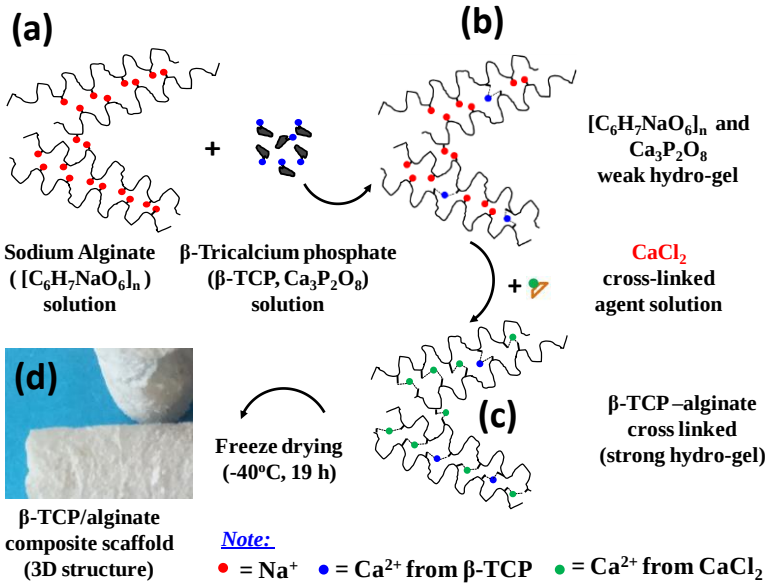

Fig. 3. A schematic reaction mechanism on the synthesis process of β-TCP/alginate composite scaffolds from β-TCP and alginate as the precursor (For interpretation of the references to colour in this figure, the reader is referred to the web version of the article).

3.3. Scaffold morphology

Macroscopic image of a selected synthesized porous β-TCP/alginate composite scaffold (Fig. 4a) clearly shows that the synthesized composite scaffold was formed in a compact shape, having several millimetre (> 10 mm) in diameter and length. From the enlarged digital photograph images in fig. 4b and 4c, it interesting to note that the composite scaffold had non uniform rough surface. In addition, for better morphology evaluation, SEM image of each composite scaffold were taken and evaluated (Fig. 5).

As can be seen in fig. 5, all synthesized composite scaffold displays interconnection pores. From fig. 5, it was observed that the synthesized TA-73 composite scaffold being the most homogeneous in term of its pore size distribution than other two composite scaffolds, indicating that the β-TCP to alginate ratio of 7:3 was found to be the most ideal pore distribution under experimental condition of this study. For biomedical application of scaffold, it has been reported that good pore uniformity properties of composite scaffolds are preferred compared to non-uniform one. Although the cell adhesion may well occur on any heterogeneous scaffold; however, a tissue formation on scaffold having non-uniform in pores size may generally lead to poor biomechanical properties [32, 33].

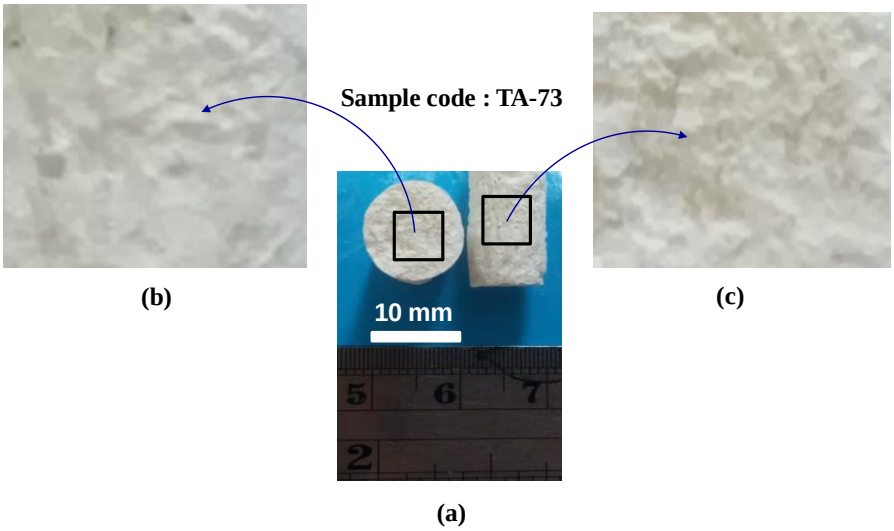

Fig. 4. Digital photograph of a selected 3D porous of β-TCP/alginate composite scaffold (For interpretation of the references to colour in this figure, the reader is referred to the web version of the article).

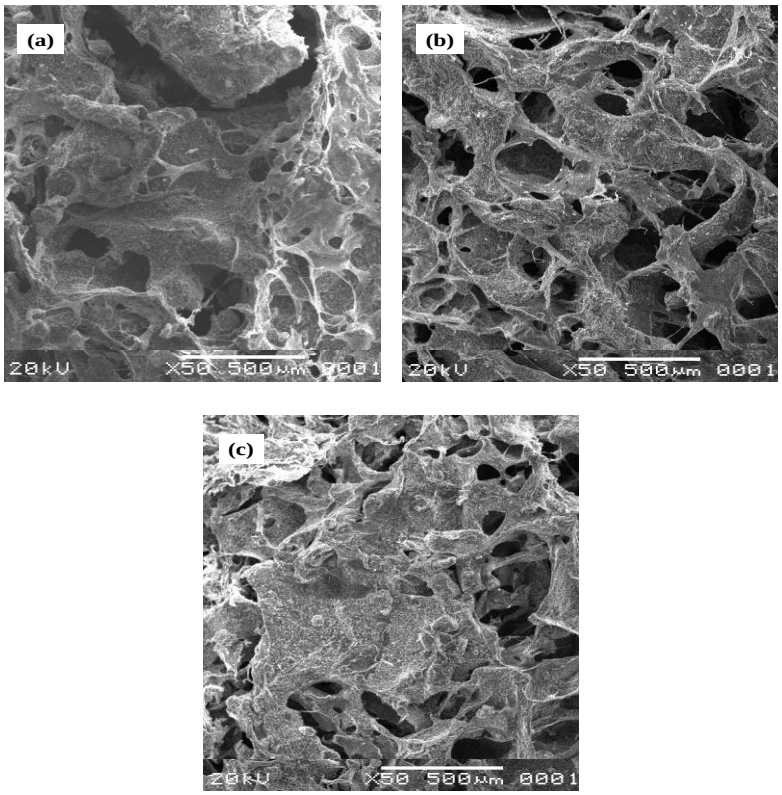

Fig. 5. SEM micrograph of porous β-TCP/alginate scaffold: a) TA-82, b) TA-73, and c) TA-64.

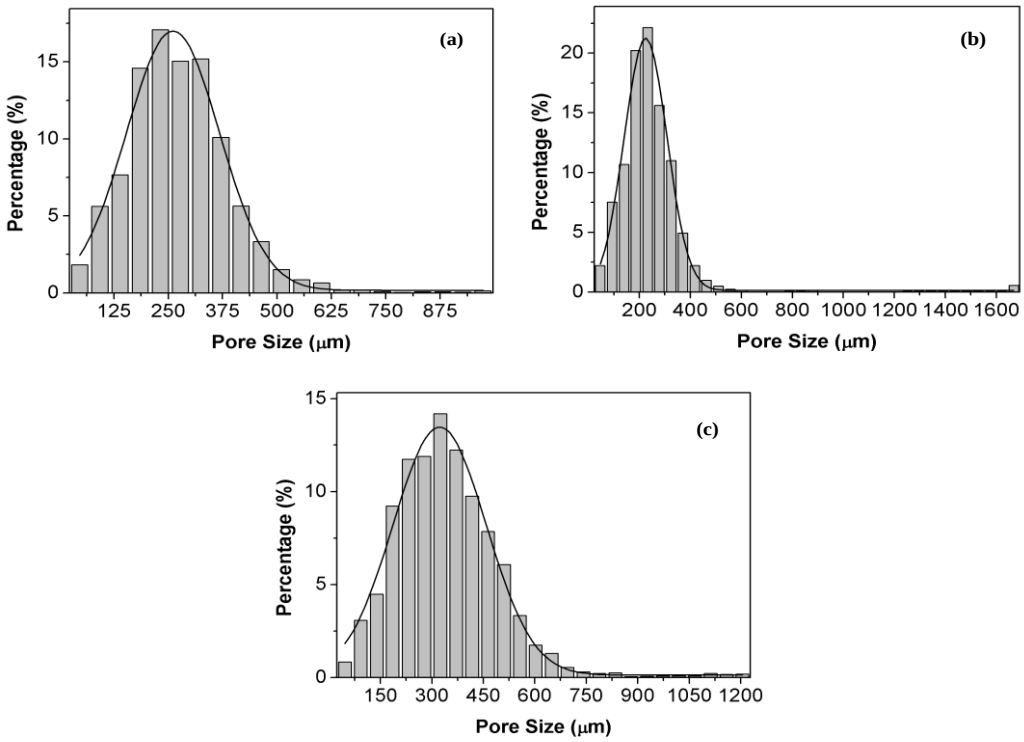

Fig. 6. Pore size distribution of β-TCP/alginate scaffold. a*) TA-82, b) TA-73, and c) TA-64.*

Fig. 6 presents a typical pore size distribution for all synthesized β-TCP/alginate composite scaffolds that were obtained by using μCT-scan. The μCT-scan data were reconstructed using software NRecon at pixel image size of 23.16 um. As it can be seen in fig. 6, the pore size distributions were found to have a Gaussian distribution function with an average pore size of the 260.8 μm, 224.2 μm and 322.3 μm for TA-82, TA-73 and TA-64, respectively. While the percentage porosity of TA-82, TA-73 and TA-64 composite scaffold was found to be 62.9, 61.6, and 68.8%, respectively. In some previous studies, it has been reported that pore size distribution for an ideal composite scaffold has to be in the range between 100 and 400 μm [3, 4]. Thus, taking the average pore size into account for those three composite scaffolds, it can be argued that all synthesized composite scaffolds obtained in this study are ideal. Specifically, the pore size distribution of the synthesized TA-73 composite scaffold (Fig. 6b) was found to be the most uniform among others. Therefore, it can be also argued that β-TCP to alginate ratio of 7:3 was an ideal one, while beyond this ratio value may lead to give less uniformity on pore size distribution. Generally speaking, non-optimum alginate addition into the β-TCP would probably lead to unevenly spread of such alginate to the β-TCP as the host matrix.

4. Conclusions

From the present study, some conclusions were pointed out. β-TCP powder can be obtained by sintering a mixture of eggshells and H_3PO_4 at 1000°C. The synthesized β-TCP powder has been successfully composed with alginate by freeze drying method using $CaCl_2$ as cross-linked to obtain a porous β-TCP/alginate composite scaffold. The freeze-drying method was found to be very suitable for synthesizing the porous β-TCP/alginate composite scaffold without phase transformation of the material before and after the freeze-drying process. Surface morphology indicates that the synthesized TA-73 was found to be most uniform in the pore size distribution compared to other synthesized composite scaffolds. However, pore size distribution of all synthesized scaffold met the requirements for ideal pore size for bone tissue engineering. According to the findings, a further detail study on the application of the synthesized β-

TCP/alginate composite scaffold for bone therapy process is very interesting to be done by our research group.

Acknowledgement

The authors gratefully acknowledge support from Indonesian Government for funding this study through Higher Education Postgraduate Scholarship-CALDOS 2013.

References

[1] A. Kolk, J. Handschel, W. Drescher, D. Rothamel, F. Kloss, M. Blessmann, M. Heiland, K. D. Wolff and R. Smeets. J. Cranio Maxill Surg. **40**, 706 (2012).
[2] C. M. Murphy, M. G. Haugh and F. J. O'Brien. Biomaterials. **31**, 461 (2010).
[3] H. Kim, G. Jung, J. Yoon, J. Han, Y. Park, D. Kim, M. Zhang and D. Kim. Mater. Sc. Eng. C. **54**, 20 (2015).
[4] A. Ogose, T. Hotta, H. Kawashima, N. Kondo, W. Gu, T. Kamura and N. Endo. J. Biomed. Mater. Res Part B: Appl. Biomater. **72B**, 94 (2004).
[5] N. Shirasu, T. Ueno, Y. Hirata, A. Hirata, T. Kagawa, M. Kanou, M. Sawaki, M. Wakimoto, A. Ota, H. Imura, T. Matsumura, T. Yamada, E. Yamachika and K. Sano. Acta Histochem. **112**(3), 270 (2010).
[6] L. Galois and D. Mainard. Acta Orthop. Belg. **70**, 598 (2004).
[7] J. Han, Z. Zhu, R. Yin, d. Yang and J. Nie. Int. J. Biol. Macromol. **46**, 199 (2010).
[8] J. Sun and H. Tan. Materials. **6**, 1285 (2013).
[9] K. Y. Lee and D. J. Mooney. Prog. Polym. Sci. **37**(1), 106 (2012).
[10] K. M. Sajesh, R. Jayakumar, S. V. Nair and K. P. Chennazhi. Int. J. Biol. Macromol. **62**, 465 (2013).
[11] M. J. Martin, A. C. Calpne, F. Fernandez, M. Malladrich, P. Galvez and B. Clares. Carbohyd. Polym. **117**, 140 (2015).
[12] J. A. Sowjanya, T. Singh, T. Mohita, S. Sarvanan, N. Srinivasan and N. Selvamurugan. Colloids Surf. B. **109**, 294 (2013).
[13] H. Jin, D. Kim, T. Kim, K. Shin, J. Jung, H. Park and S. Yoon. Int. J. Biol. Mol. **51**, 1079 (2012).
[14] X. He, R. Dziak, K. Mao, R. Genco, M. L. C. Swithart and S. Yang. Tissue Eng. Part A. **19**, 1 (2012).
[15] G. Tripathi and B. Basu. Ceramics Int. **38**, 341 (2012).
[16] F. Scalera, F. Gervaso, K. P. Sanosh, A. Sannino and A. Licciulli. Ceram. Int. **39**, 4839 (2013).
[17] E. B. Montufar, T. Traykova, C. Gil, A. Harr, A. Almirall, A. Aguirre, E. Engel, J. A. Planell M. P. Ginebra. Acta Biomater. **6**, 876 (2010).
[18] M. H. Nazarpak and F. Pourasgari. Int. J. Biosci. Biochem. Bioinforma. **4**(3), 142 (2014).
[19] S. Deville. Materials. **3**, 1913 (2010).
[20] BPS. Produksi Telur Unggas dan Susu Sapi Menurut Provinsi. Available: http://www.bps.go.id/, (Accessed 1 Agustus 2015).
[21] K. S. TenHusein and P. W. Brown. J. Am. Ceram. Soc. **82**, 2813 (1999).
[22] O. Zuas, H. Abimanyu, W. Wibowo. Proc. Appl. Ceram. **8**(1), 39 (2014).
[23] I. Nikevic, D. Maravic, N. Ignjatovic, M. Mitric, D. Makovec and D. Uskokovic. Mater. Trans. **47**(12), 2980 (2006).
[24] J. I. M. Alvarez and G. H. Carmona. J. Appl. Phycol. **19**, 54 (2007).
[26] C. Sartori, D. S. Finch, B. Ralph and K. Giding. Polymer. **38**(1), 43 (1997).
[27] L. B. Cimdina and N. Borodajenko, in *Research of Calcium Phosphate Using Fourier Transform Infrared Spectroscopy*, edited by T. Theophanides. Materials, Science, Engineering, and Technology. INTECH. Croatia.
[28] M. K. Narbat, F. Orang, M. S. Hashtjin and A. Goudarzi. Iranian Biomed. J.

10(4), 215 (2006).
[29] E. M. Rivera, M. Araiza, W. Brostow, V. M. Castano, J. R. Estrada, R. Hernandez, J. R. Rodriguez. Mater. Lett. **41**, 128 (1999).
[30] N. Jinlong, Z. Zhenxi and J. Dazong. J. Mater. Synt. Proces. **9**(5), 235 (2002).
[31] S. Fu, A. Thacker, D. M. Sperger, R. L Boni, I.S. Buckner, S. Velankar, E.J. Munson, L.H. Block. AAPS Pharm. Sci. Tech. **12**(2), 453 (2011).
[32] G.T. Grant, E.R. Morris, D.A. Rees, P.J.C. Smith, D. Thom. FEBS Lett. **32**(1), 195 (1973).
[33] F. J. O'Brien, B. A. Harley, I. V. Yannas and L. Gibson. Biomaterials. **25**, 1077 (2004).
[34] S. J. Hollister, R. D. Maddox and J. M. Taboas. Biomaterials. **23**, 4095 (2002).